의학석사 학위논문

Quantification of Macular Ellipsoid Zone Intensity in Glaucoma Patients

녹내장 진행 정도에 따른 황반부 타원체영역 반사강도 정량화에 관한 연구

2019년 8월

서울대학교 대학원

의학과 안과학 전공

하 아 늘

A thesis of the Degree of Master of Medical Science

Quantification of Macular Ellipsoid Zone Intensity in Glaucoma Patients

녹내장 진행 정도에 따른 황반부 타원체영역 반사강도 정량화에 관한 연구

August 2019

The Department of Ophthalmology
Seoul National University
College of Medicine
Ahnul Ha

ABSTRACT

Quantification of Macular Ellipsoid Zone Intensity in Glaucoma Patients

Ahnul Ha

Department of Ophthalmology

The Graduate School

Seoul National University College of Medicine

Purpose: 1) To compare retinal photoreceptor ellipsoid zone (EZ) intensity between normal eyes and those with different stages of glaucoma. 2) To describe an automated method (AM) for quantification of macular EZ intensity (mEZi) and to compare its performance with a manual method (MM) from glaucoma patients and healthy controls.

Methods: 71 patients with mild-to-moderate glaucoma (mean age 58 ± 12), 71 patients with severe glaucoma (mean age 60 ± 13), and 51 controls (mean age 60 ± 11) were enrolled in a clinical setting. The subjects underwent high-resolution 9-mm-length horizontal and vertical line scans through the fovea by spectral-domain optical coherence tomography (SD-OCT). 1) In 37 normal, 38 preperimetric glaucoma, 39 mild-to-moderate glaucoma (visual field [VF] mean deviation [MD]: -7.7 ± 2.0 dB), and 36 severe glaucoma eyes (VF MD: -17.8 ± 3.2 dB), the relative EZ intensity as the ratio of the second to first reflective band (EZ/ELM) was determined by MM. 2) Calibration (n = 160) and validation (n = 33) images sets were assembled. Correlation between AM and MM quantification was assessed by Deming regression within the calibration set and a compensation formula was generated to account for the subtle, systematic differences. Then, compensated AM quantification for each validation images sets were compared with the mean and 95% confidence interval of five MM quantification of the validation set performed by a single observer.

Results: 1) The relative EZ intensity in severe glaucoma eyes was significantly lower than in mild-to-moderate glaucoma eyes (2.46 ± 0.38 vs 3.15 ± 0.43, $P < 0.001$); also, it was lower in mild-to-moderate than in preperimetric glaucoma eyes (3.15 ± 0.43 vs 3.86 ± 0.44, $P < 0.001$). However, the comparison between preperimetric glaucoma and normal eyes showed no significant difference (3.86 ± 0.44 vs 4.06 ± 0.40, $P = 0.751$). In 75 glaucomatous eyes with VF defect, there was a significant correlation between relative EZ intensity and VF MD (r = 0.83 and $P < 0.001$). 2) AM quantification linearly correlated to MM quantification in both calibration and validation sets ($R^2 = 0.991$, $P < 0.001$ and $R^2 = 0.942$, $P < 0.001$). In the validation set, compensated AM quantification fell within the 95% confidence interval of the MM quantification in 32 of the 33 images sets (96.97%).

Conclusions: According to SD-OCT, relative EZ intensity reduction occurs in the mild-to-moderate and severe glaucoma stages. These findings suggest, at least provisionally, that in the course of glaucoma progression, mitochondrial changes in the inner segments of photoreceptors occur. In addition, an AM for mEZi quantification has been calibrated and validated relative to MM quantification in both glaucoma patients and healthy controls.

……

Keywords: Macular Ellipsoid Zone Intensity, Automated Quantification, Calibration and Validation, Optical Coherence Tomography, Glaucoma.

***Student Number*:** 2017-29480

CONTENTS

LIST OF TABLES AND FIGURES

LIST OF ABBREVIATIONS

RGCs, retinal ganglion cells

SD-OCT, spectral-domain optical coherence tomography

EZ, ellipsoid zone

mEZi, macular EZ intensity

AM, automated method

MM, manual method

D, diopters

VF, visual field

SDP, stereo disc photography

RNFL, retinal nerve fiber layer

HVF, Humphrey Visual Field

MD, mean deviation

ELM, external limiting membrane

TIFF, tagged image file format

SD, standard deviation

I. Introduction

Glaucoma manifests as pathological changes in the inner retina's retinal ganglion cells (RGCs).[1, 2] It has been observed that degenerative changes in the lateral geniculate nucleus and visual cortex can co-present in glaucomatous eyes by trans-synaptic degeneration and that they occur in relation to the severity of RGCs cell loss.[3] The mechanisms underlying the processes are not yet exactly known, but based on the fact that retinal neuronal cells are closely related both structurally and functionally, it has been posited that outer-retinal-layer changes might occur as well, according to similar principles. In fact, impaired outer-retinal neuronal function as well as cell-number reduction in the photoreceptor layer have been demonstrated in glaucomatous eyes.[4-7]

Imaging equipment and software advances, meanwhile, have enabled analysis of the outer-retinal structure in greater detail. Spectral-domain optical coherence tomography (SD-OCT), for example, is a noninvasive imaging modality providing in vivo images that are comparable to histological samples, and with good reproducibility as well.[8] SD-OCT also facilitates accuracy, repeatability, and precision in the delineation of individual retinal layers, thereby providing the opportunity for identification of structural biomarkers of varing disease severity.[9]

The outer retina's second hyper-reflective band on SD-OCT is a known marker of disease severity in a number of diverse retinal diseases such as age-related macular degeneration and inflammatory disease.[10-13] Whereas traditionally it has been associated with the photoreceptors' inner/outer segment junction, more recent studies suggest an anatomical correlation with the inner-segment ellipsoid, which, by international nomenclature consensus, is referred to as the ellipsoid zone (EZ).[14, 15] The EZ, as it is densely packed with mitochondria, is essential to photoreceptors' structural integrity and function; indeed, it has

important metabolic and light-guiding roles.[16, 17] Observation of EZ changes in glaucoma patients, then, has the potential to provide clues to outer-retinal involvement in glaucoma.

Hood et al.[18] demonstratred an intensity reduction (albeit associated with a band relatively normal in appearance) of EZ band in patients suffering diminished photoreceptor cone function. Gin et al.[12] suggested, for analysis of EZ band intensity on SD-OCT, a quantitiative measurement method. Thus prompted, in the present study, we performed an SD-OCT comparative assessment of EZ intensity between glaucoma patients at different disease stages and normal subjects. In addition, we describe the methodological approach and demonstrate the results of automated strategy for quantification of macular EZ intensity (mEZi). Automated method (AM)'s performance is compared with a manual method (MM) from glaucoma patients and healthy controls. Our data will provide a starting point for future longitudinal studies seeking to demonstrate an EZ-change time course for glaucoma advance.

CHAPTER 1. Ellipsoid Zone Change according to Glaucoma-Stage Advancement

II. Methods

This study was approved by the Seoul National University Hospital Institutional Review Board and faithfully adhered to the tenets of the Declaration of Helsinki.

1. Study Subjects

All of the study subjects were examined between January 2015 and October 2017 at the Seoul National University Hospital Glaucoma Clinic in Seoul, Korea. Based on a retrospective review of medical records, eligible participants were consecutively enrolled. All were subjected to a complete ophthalmic examination, including visual acuity assessment, refraction, slit-lamp biomicroscopy, gonioscopy, Goldmann applanation tonometry (Haag-Streit, Koniz, Switzerland), and dilated stereoscopic examination of the optic disc. Additionally, the subjects underwent the following: central corneal thickness measurement (Orbscan 73 II, Bausch & Lomb Surgical, Rochester, NY, USA), axial length measurement (IOL Master ver. 5, Carl-Zeiss Meditec, Dublin, CA, USA), stereo disc photography (SDP), red-free retinal nerve fiber layer (RNFL) photography, Cirrus HD-OCT (Carl Zeiss Meditec, Inc., Dublin, CA) including macular ganglion cell-inner plexiform layer (GCIPL) thickness and central 30-2 threshold testing of the Humphrey Visual Field (HVF) (HFA II; Humphrey Instruments Inc., Dublin, CA).

For inclusion in the study, subjects were required to be aged between 40 and 65 years, to have a best-corrected visual acuity greater than or equal to 20/40 in the Snellen equivalent, a spherical refraction greater than -6 diopters (D) and less than 3 D, an open anterior chamber angle, and reliable results on visual-field (VF) tests. The exclusion criteria

were as follows: (1) a history of intraocular surgery (except uncomplicated cataract surgery) or retinal laser photocoagulation and (2) any neurological and systemic diseases potentially affecting retinal structure and/or function and VF results. Additionally excluded were any cases of suspicious retinal lesions possibly affecting the outer-retinal layer, including inflammatory conditions as well as hereditary and degenerative retinal diseases.

Glaucomatous eyes were defined based on the appearance of the characteristic optic disc (localized or diffuse neuroretinal rim thinning/notching) on SDP and the presence of RNFL defect in the corresponding region on red-free fundus imaging, regardless of the presence or absence of glaucomatous VF defect. Signs of optic disc on SDP and of RNFL on red-free imaging were independently evaluated by two glaucoma specialists (AH and KHP) masked to all other clinical data. Discrepancies between their findings were resolved by consensus. Among the glaucomatous eyes, the pre-perimetric glaucoma diagnosis was made in cases of a normal VF on conventional HVF. Normal HVF results were defined as mean deviation (MD) and pattern standard deviation within the 95% confidence limits and a glaucoma hemifield test result within the normal limits.

Glaucomatous VF defects were defined as follows: (1) a cluster of 3 points with probabilities less than 5% in at least 1 hemifield on the pattern deviation map, including at least 1 point with a probability less than 1% or a cluster of 2 points with a probability less than 1%, (2) Glaucomatous Hemifield Test results outside the normal limits, or (3) a pattern standard deviation beyond 95% of the normal limits, as confirmed by at least 2 reliable examinations (false-positive/negatives <15%, fixation losses <15%). Based on a reliable HVF result obtained on the day of SD-OCT imaging, the glaucoma patients were divided into three groups: pre-perimetric glaucoma (no glaucomatous VF defect), mild-to-moderate glaucoma (VF MD $\geq$ -12 dB), and severe glaucoma (VF MD < -12 dB).

The normal controls had an intraocular pressure (IOP) less than or equal to 21 mm

Hg, no history of IOP elevation, no glaucomatous optic disc appearance, no RNFL/GCIPL defect, and normal HVF results. If both eyes were found to be eligible, one was selected randomly.

2. Imaging of Outer-Retinal Layer

All of the subjects were scanned by SD-OCT confocal scanning laser ophthalmoscopy (Spectralis HRA+OCT; Heidelberg Engineering, Heidelberg, Germany) using the eye-tracking feature (TruTrack; Heidelberg Engineering, Heidelberg, Germany). All imaged were obtained through dilated pupils by a single experienced examiner. Two 9-mm line scans, one along the horizontal meridian and the other along the vertical meridian, were obtained with the high-resolution setting, and the images of 128 frames centered on the fovea were averaged. The presence of the foveal bulge, foveal depression, and inner-retinal-layer thinning, all as seen on SD-OCT, was taken as confirmation of the foveal area. To be included, all images were reviewed for non-centered scans or presence of artifacts, and had a signal quality > 20 dB.

3. Manual EZ Intensity Quantification Method

EZ is known to become less distinct with eccentricity. The mitochondrial packing density in the ellipsoid is lower for rods than for cones, and the proportion of the area occupied by rods increases with eccentricity.[14] Further, the inner segments of the cones become shorter and wider towards the periphery of the retina, resulting in a blurred EZ boundary.[14] In a previous study, EZ remained consistent until about 10° (3000 μm) peripheral from the fovea. Near the 12° (3600 μm) periphery, the EZ and interdigitation zone approached one another and became indistinguishable.[19] Likewise, according to the results of our pilot study on 25 normal and 25 glaucoma eyes, the maximum range in which clear and reliable EZ intensity can be obtained was about 2000 μm from the fovea. In this study, therefore, for the purpose of consistent and accurate EZ intensity measurements, we analyzed only the central macular

area (total 4000 μm-length). To account for OCT-scan brightness variation, the relative EZ intensity was determined as the ratio of the second reflective band to the first (i.e., the EZ/external limiting membrane[ELM] ratio). The ELM was used as the anatomic reference for EZ intensity calculation, as it is a non-neural layer maintaining a constafiguret intensity regardless of age or retinal degeneration stage.[14, 20] ELM intensity across a wide eccentricity is considered to be relatively constant.[21]

Logarithmic-transformed B-scans (horizontal and vertical SD-OCT line scans through the fovea) for each eye of each participant were analyzed and displayed in tagged image file format (TIFF). The relative EZ intensity in each quadrant (superior, temporal, inferior, and nasal) of 4000-μm horizontal and vertical retinal scans through the fovea was averaged, each meridian consisting of 20 retinal segments and one central (C) segment, as shown in Figure 1. Notably, the EZ and ELM were not always parallel to the OCT scan's horizontal plane; thus, for the purpose of consistent and accurate intensity measurements, it was necessary to divide each cross-sectional image into several small segments. Through preliminary validation confirming the optimal number and width of the segments, the method for analyzing an EZ of total 4000 μm-length in 150 μm-width segments (resulting in 21 200-μm-interval retinal segments) was determined, and the rectangular segments utilized for intensity analysis were drawn perpendicularly to the EZ and ELM but not to the OCT horizontal plane.

Relative EZ intensity was measured as the highest EZ band intensity value divided by the highest ELM band intensity value of the SD-OCT images (see Figure 1). All of the measurements were performed using the public-domain NIH Image program (ImageJ 1.48v, Wayne Rasband, National Institutes of Health, Bethesda, MD, USA). To avoid the local ''shadowing'' effects of retinal vessels on the EZ and ELM intensity, any segments exhibiting this effect were excluded from further analysis. An experienced ophthalmologist (YKK) blinded to the patients' clinical information performed all of the intensity measurements.

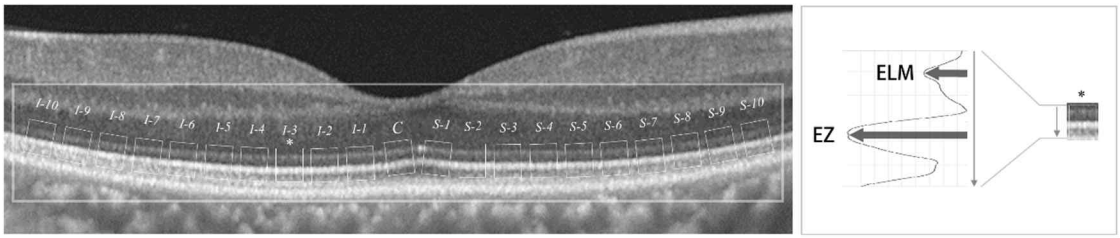

Figure 1. Illustrative diagram of 21 retinal locations of ellipsoid zone (EZ) and external limiting membrane (ELM) sampling at fovea and to maximum 2000 μm eccentricity from fovea, vertically. Each sample was 150 μm in width and had 200 μm of interval. Accordingly, the "relative intensity of an EZ segment" was taken as the EZ segment intensity divided by the ELM intensity. The retinal segment (I-3) used for relative EZ intensity calculation is marked with asterisks.

4. Statistical Analysis

Comparison of the normally distributed demographic data and relative EZ intensities among the four groups (i.e., normal group, three glaucoma [pre-perimetric, mild-to-moderate, severe] groups) was performed by one-way analysis of variance with Tukey's post-hoc test. The categorical data were analyzed by χ^2 test with Bonferroni correction for multiple comparisons. For glaucomatous eyes, Pearson correlation analysis of the relative EZ intensity with VF MD was performed. In all of the analyses, parametric or nonparametric tests were utilized based on the normality test, and 95% confidence interval (CI) was calculated. Statistical analysis was performed using the SPSS statistical package (SPSS 22.0; Chicago, IL, USA), and a *P* value less than 0.05 was considered statistically significant

III. Results

A total of 179 eyes (179 subjects) meeting the entry criteria underwent SD-OCT. Twenty-nine (29) eyes (29 subjects) were excluded due to poor-quality OCT scans. A total of 37 normal eyes (37 subjects), 38 pre-perimetric glaucomatous eyes (38 subjects), and 75 glaucomatous eyes with VF defect on HVF (75 subjects) were included. All of the enrolled subjects were primary open-angle glaucoma (POAG) patients with untreated IOP ≤ 21 mmHg (i.e., normal-tension glaucoma [NTG] patients). The glaucomatous eyes with VF defect were subdivided as follows: 39 eyes with mild-to-moderate glaucoma (VF MD ≥ -12 dB) and 36 eyes with severe glaucoma (VF MD < -12 dB).

1. Demographic and Clinical Characteristics of Study Subjects

The demographic characteristics along with the systemic and ocular factors for each group are summarized in the Table 1. The four groups' mean age, gender distribution, IOP at time of OCT measurement, central corneal thickness, spherical equivalent, axial length and lens status were similar (P = 0.469, 0.467, 0.140, 0.609, 0.641, 0.145, and 0.954 respectively). Average GCIPL thickness and VF MD significantly differed across all four groups (P < 0.001, respectively).

Table 1. Demographic and Baseline Clinical Characteristics of Study Patients

		Glaucoma			
	Normal *N* = 37	Pre-perimetric *N* = 38	Mild-to-Moderate *N* = 39	Severe *N* = 36	*P*
Baseline Factors					
Age (yrs)	57.03 ± 5.38	57.95 ± 6.90	59.10 ± 6.66	59.06 ± 7.00	0.469[a]
Male, n (%)	21 (57)	20 (53)	23 (59)	21 (58)	0.467[b]
Systemic Factors					
Diabetes mellitus, n (%)	4 (11)	4 (11)	5 (13)	4 (11)	0.989[b]
Hypertension, n (%)	6 (16)	7 (18)	6 (15)	6 (17)	0.987[b]
Cardiovascular disease, n (%)	3 (8)	4 (11)	4 (10)	4 (11)	0.976[b]
Ocular factors					
IOP (mmHg)	12.19 ± 1.61	13.08 ± 1.94	12.03 ± 1.83	12.06 ± 2.41	0.140[a]
Central corneal thickness (μm)	533.82 ± 23.12	531.24 ± 29.21	528.31 ± 35.32	524.56 ± 33.97	0.609[a]
Spherical equivalent (diopters)	-0.16 ± 1.81	0.00 ± 1.49	-0.36 ± 2.21	-0.32 ± 1.90	0.641[a]
Axial length (mm)	24.08 ± 1.40	23.44 ± 1.00	23.78 ± 1.32	23.91 ± 1.13	0.145[a]
Lens status, pseudophakic, n (%)	12 (32)	13 (34)	15 (39)	13 (36)	0.954[b]
Average GCIPL thickness (μm)	82.82 ± 8.41	78.62 ± 7.31	69.53 ± 4.01	60.93 ± 5.76	< 0.001[a]
VF MD (dB)	-0.23 ± 0.58	-0.88 ± 0.58	-7.67 ± 1.94	-17.77 ± 3.22	< 0.001[a]

IOP, intraocular pressure; GCIPL, ganglion cell-inner plexiform layer; VF MD, visual field mean deviation.
Values are shown as mean ± standard deviation unless otherwise indicated.
[a]One-way analysis of variance, [b]Chi-square test with Bonferroni correction.

2. Comparison of Relative EZ Intensity between Normal Subjects and Eyes with Different Stages of Glaucoma

The relative EZ intensity did not show a statistically significant difference between the normal and pre-perimetric glaucomatous eyes (4.06 ± 0.40, CI 3.92-4.19 vs. 3.86 ± 0.44, CI 3.71-4.00, $P = 0.751$). However, the relative EZ intensities were significantly reduced in glaucomatous eyes with VF defect, both in the mild-to-moderate glaucoma group (3.15 ± 0.43, CI 3.02-3.30, $P < 0.001$) and in the severe glaucoma group (2.46 ± 0.38, CI 2.33-2.59, $P < 0.001$) relative to the normal subjects; meanwhile, the relative EZ intensity was much lower in the severe glaucoma group than in the mild-to-moderate glaucoma group ($P < 0.001$, Figure 2).

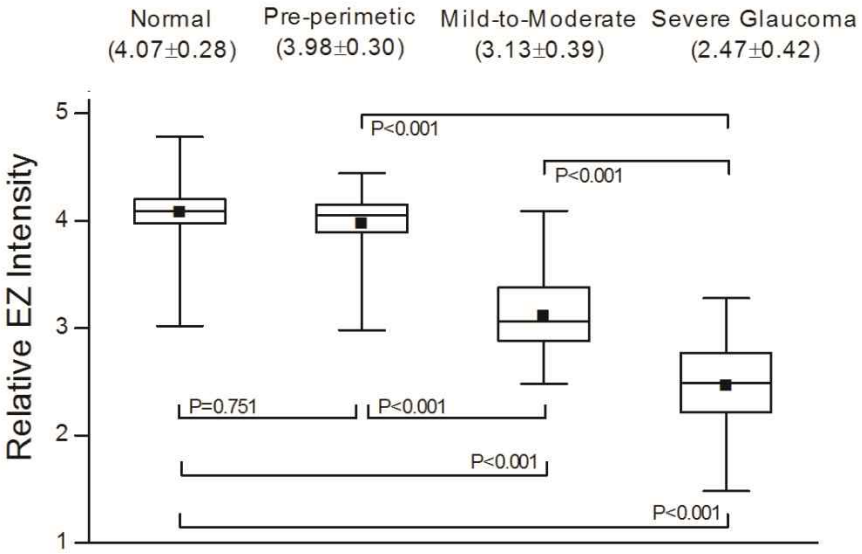

Figure 2. Box-and-Whisker plot of relative EZ intensity in each group. The relative EZ intensity was significantly reduced in the mild-to-moderate and severe glaucoma groups ($P < 0.001$); however, no significant EZ intensity reduction was observed in the pre-perimetric group relative to the normal group ($P = 0.751$). Black squares in the box, lines of the ends of the box and two lines outside the box represent the means, upper/lower quartiles and maximum/minimum values, respectively.

3. Relationship of Relative EZ Intensity to VF MD

The relative EZ intensity of 75 glaucomatous eyes with VF defect were plotted against their VF MD (Figure 3). The relative EZ intensity and VF MD showed a statistically significant correlation ($r = 0.850$, $P < 0.001$) and, the correlation remained statistically significant after controlling for age ($r = 0.830$, $P < 0.001$). The correlation between relative EZ intensity and VF MD was statistically significant in all three glaucoma groups with and without VF defects ($r = 0.357$; $P = 0.030$, $r = 0.644$; $P < 0.001$ and $r = 0.732$; $P < 0.001$, respectively).

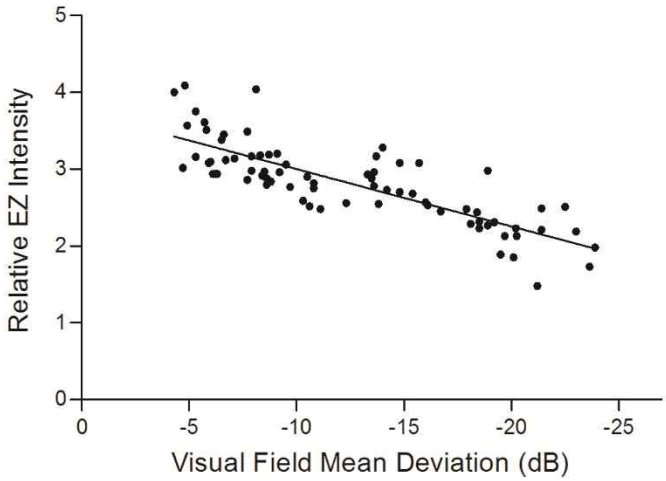

Figure 3. Scatter plots of relative EZ intensity against visual field mean deviation (VF MD) in glaucomatous eyes with visual field defect. In 75 glaucomatous eyes with VF defect (i.e., the mild-to-moderate and severe glaucoma groups), the relative EZ intensity showed a statistically significant correlation with VF MD ($r = 0.830$, $P < 0.001$ after controlling for age).

IV. Discussion

Having performed an in vivo evaluation of the outer retina at different stages of glaucoma, we found that EZ intensity reduction on SD-OCT occurs in the mild-to-moderate and severe glaucoma stages. To our best knowledge, this is the first report to examine EZ intensity change on SD-OCT according to glaucoma-stage advancement.

The histologic data gathered in the relevant previous studies have suggested that the EZ consistently aligns with the photoreceptors' inner-segment ellipsoids that consist of tightly packed mitochondria.[14] Thus, EZ reflectivity might, at least in part, represent the integrity of mitochondria in photoreceptors.[10] In age-related macular degeneration, in the pathogenesis of which the mitochondria-related pathways play a key role, EZ band intensity has been found to be significantly lower than in control subjects of a similar age.[13] In another study, reduced EZ intensity was significantly associated with multifocal electroretinogram implicit time delay indicative of decreased retinal function.[21] In the present study, there was a significant correlation between relative EZ intensity and glaucoma severity: with greater glaucomatous VF damage, EZ intensity was further reduced. On this basis, we may posit that the mitochondria in the inner segments of photoreceptors might be affected in the course of glaucoma progression.

One possible explanation of the EZ intensity reduction mechanism is trans-synaptic degeneration occurring after RGC loss in glaucomatous eyes. Anatomically, RGC dendrites form synapses to the bipolar and amacrine cells, which inter-neurons connect to the photoreceptors.[22] Neurons can affect other synapsed neurons, either directly or indirectly, by retrograde or anterograde degeneration.[23] In the central nervous system, retrograde trans-synaptic degeneration of the optic nerve and ganglion cells has been noted after occipital lesions.[24, 25] Embryological findings supporting the presence of centrifugal (i.e. brain-to-retina) fibers along with physiological evidence of impulses conveyed along those centrifugal fibers have been revealed.[26, 27] Gills et al.[28] showed that significant trans-synaptic

degeneration also can occur in the inner nuclear layer of the retina following the optic nerve lesions. Progressive retinal thinning consequent upon brain damage due to stroke in the corresponding region has been demonstrated using SD-OCT ganglion-cell-layer analysis.[29] Likewise, it has been posited that retrograde trans-synaptic degeneration can take place within the photoreceptors after extensive RGC loss.[30]

There have been conflicting reports on the retrograde trans-synaptic degeneration effect of RGCs damage on the outer retina. One of the causes of such inconsistency can be the differing densities of the synapses connected to RGCs and photoreceptors.[22] It is possible that the outer-retinal cells are less prone to retrograde trans-synaptic degeneration due to the fact that they have more collateral neural connections (as has been shown for polyaxonal amacrine cells in the rabbit retina)[31, 32] that can guarantee greater supply of neurotrophic factors to the neurons. Additionally, the process of retrograde trans-synaptic degeneration is known to be very slow, especially in higher-developed animal species,[33] and this might explain the lack of awareness of its clinical significance until now. Furthermore, in most of the previous animal experiments, neurons have been mainly investigated by histology though metabolic or functional changes can precede actual morphologic alterations to cells, thus masking evidence of retrograde trans-synaptic degeneration in photoreceptors.

Further, RGCs are in close contact with glial cells, of which there are three (3) types: Müller cells, astrocytes, and microglia. Under normal conditions, glial cells support neuronal function of photoreceptors via a variety of structural and nutritional mechanisms.[34] At some point though, a shift in cell function, perhaps triggered by the prolonged stress that is associated with glaucomatous change, seemingly occurs, after which cells are no longer supportive but damaging to neuronal tissue.[35] In such circumstances, glial cells become neuro-destructive, thereby releasing increased amounts of neurotoxic substances such as tumor necrosis factor-alpha (TNF-α) and nitric oxide.[23] Generalized loss of astrocyte coverage over the RNFL, and the resultant dysregulation of vascular permeability and

endothelial cell activation, have been demonstrated by a rodent experimental model of glaucoma.[36] These alterations in the function of glial cells are expected to cause structural and functional changes in photoreceptor cells. Indeed, based on our results, it can be deduced that advanced glaucoma's discursive damage to RGCs and prolonged stress on glial cells can potentially affect the EZ of the outer-retinal layer.

It is known that choroidal hypoperfusion is associated, to some extent, with glaucoma's pathophysiology. Spraul et al.'s histological study found that post-mortem eyes manifesting severe glaucomatous damage after long-standing POAG showed a lower-density choriocapillaris at the macula relative to control eyes.[37] By both histological and angiographic techniques, significantly reduced choroidal thickness, delayed peak choroidal filling, decreased vessel frequency and smaller mean vessel diameter have been identified in POAG eyes.[38] Given the outer retina's utter dependence on the choriocapillaris for its very high oxygen-consumption requirement,[39] lowered choriocapillary blood-supply could lead to outer-retinal ischemia in advanced stages of POAG, which might, in turn, affect the EZ (i.e., mitochondria) in the photoreceptor's inner segments.

Interestingly, no EZ intensity reduction was observed in glaucomatous eyes at the pre-perimetric stage. Werner et al.[40] demonstrated that outer-retinal cell loss occurs in cases manifesting long-term visual field loss, on which basis they suggested that outer-retinal-structural changes lag cell loss in the inner retina. This means that RGC damage exceeding a certain critical point can have a negative effect on photoreceptors. Also, a cell-function shift from neuro-protection to neuro-destruction of glial cells has been known to occur only when prolonged stress exceeds a specific point. These results indicate that in early stages of glaucoma at which substantial numbers of RGCs survive, photoreceptor cell functionality might not yet be significantly affected.

The present study's findings must be interpreted in light of its limitations. First, we defined the ELM as a reference structure, as it does not significantly differ with either age or

glaucomatous change.[41] However, we cannot rule out the possibility that subtle ELM intensity changes resulting from undiagnosed pathologies affected our results. Second, artifacts or posterior vitreous detachment can lead to focal intensity change on SD-OCT images. For minimization of this effect, we verified all images manually prior to the intensity analysis in order to identify any conditions possibly affecting the outer retina. Third, intensity was measured within the central 4000 x 4000-μm area, because the ELM and EZ tend to show less clear boundaries toward the periphery on OCT images. Considering the fact that, in glaucoma progression, arcuate defects generally occur first, it is possible that our EZ intensity results would have shown decreases from the earlier disease stage if we had included the intensity values of the more peripheral areas. Further, in order to obtain more accurate and consistent EZ intensity data, the average EZ intensity values of multiple scans within the area of interest should be calculated. Fourth, it is possible that our observation of "no change" in EZ intensity in the early stage of glaucoma was due to the current image modality's lack of sufficient sensitivity to detect such change. Finally, this was a cross-sectional study. A future longitudinal study should be conducted to investigate any correlations of outer-retinal-layer change with glaucomatous optic neuropathy progression.

In conclusion, relative EZ intensity reduction in the mild-to-moderate and severe glaucoma stages was found on SD-OCT, and the extent of reduction was positively associated with glaucoma severity. These findings tentatively suggest that secondary changes to mitochondria that are packed tightly within photoreceptors' inner-segment ellipsoids might occur during glaucoma progression. The clinical significance of potential EZ intensity reduction in glaucoma should be further evaluated.

CHAPTER 2. Automated Quantification of Macular Ellipsoid Zone Intensity

II. Methods

1. Overview of Study Design

First, a calibration study was performed to compare mEZi by each method (AM or MM) within an initial group of 160 images sets. These images were obtained from normal (n = 40), mild-to-moderate glaucoma (n = 60), and severe glaucoma (n = 60) eyes in order to balance from each damage level. Next, a validation study was performed to compare AM quantification with the MM quantification by assessing whether the AM quantification fell within the range of repeated MM quantification. For this experiment, MM quantification were repeated five individual times on a separate group of 33 images sets representing a similar, broad range of glaucomatous damage (11 images per group). The AM quantification were compared with the mean MM quantification and with the range of MM re-quantify variability (95% confidence interval). Finally, to demonstrate the overall strategy for automated mEZi quantification, OCT image acquisition, and AM mEZi measurement were described for the macular area of the normal and glaucoma eyes.

2. Study Subjects

All of the study subjects were examined between January 2015 and December 2018 at the Seoul National University Hospital Glaucoma Clinic in Seoul, Korea. Based on a retrospective review of medical records, eligible participants were consecutively enrolled. For inclusion in the study, subjects were required to be aged between 40 and 65 years, to have a spherical refraction greater than -6 D and less than 3 D, an open anterior chamber angle, and reliable results on VF tests. The exclusion criteria were as follows: (1) a history of intraocular surgery (except uncomplicated cataract surgery) or retinal laser photocoagulation and (2) any

neurological and systemic diseases potentially affecting retinal structure and/or function and VF results. Additionally excluded were any cases of suspicious retinal lesions possibly affecting the outer-retinal layer, including inflammatory conditions as well as hereditary and degenerative retinal diseases.

Glaucomatous eyes were defined based on the appearance of the characteristic optic disc (localized or diffuse neuroretinal rim thinning/notching) on SDP and the presence of RNFL defect in the corresponding region on red-free fundus imaging. Signs of optic disc on SDP and of RNFL on red-free imaging were independently evaluated by two glaucoma specialists (AH and KHP) masked to all other clinical data. Discrepancies between their findings were resolved by consensus. Based on a reliable HVF C30-2 result, the glaucoma patients were divided into two groups: mild-to-moderate glaucoma (VF MD ≥ -12 dB) and severe glaucoma (VF MD < -12 dB). The normal controls had an IOP less than or equal to 21 mm Hg, no history of IOP elevation, no glaucomatous optic disc appearance, no RNFL defect, and normal HVF results. If both eyes were found to be eligible, one was selected randomly.

3. Automated EZ Intensity Quantification Method and Software Application

AM was developed that, given an image, provides an average of relative mEZi (i.e., the EZ/ELM ratio) in the horizontal and vertical line scans. In each line scan, the mEZi was quantified in 200 sectors evenly spaced. In one eye, therefore, the mEZi were quantified in about 400 sectors. The AM was based on Python programming, and used Opencv library for image processing. The details of automated mEZi quantification methods were as follows. First, it crops the macular image according to the pixel numbers (threshold 50,250) to detect the center (Figure 4A-B). Second, within the central 4000-μm area, inner retinal layer structures were eliminated by brightness thresholding (threshold 160,250, Figure 4C-D). This process leaves only the three bright layers (i.e., EZ, interdigitation zone, and retinal pigment

epithelium) in the outer retinal layer (Figure 4D). Then, the region above 15 pixels from EZ was defined as the upper boundary to include ELM. The regions of interest (ROI) image (Figure 4E) was multiplied by this binary masked image to extract outer retinal layers including both ELM and EZ (Figure 4F). Finally, by calculating the ratio of the intensity peaks by EZ and ELM, mEZi was determined (Figure 4G). For details on the algorithm and process of the AM, refer to Figure 5.

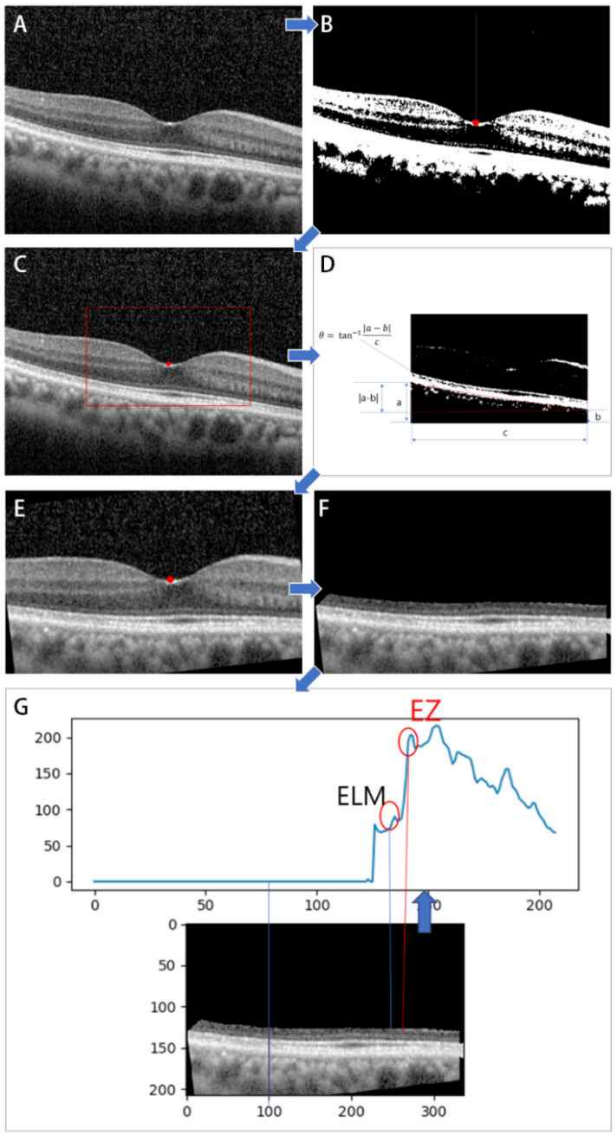

Figure 4. The process of mEZi quantification via AM.

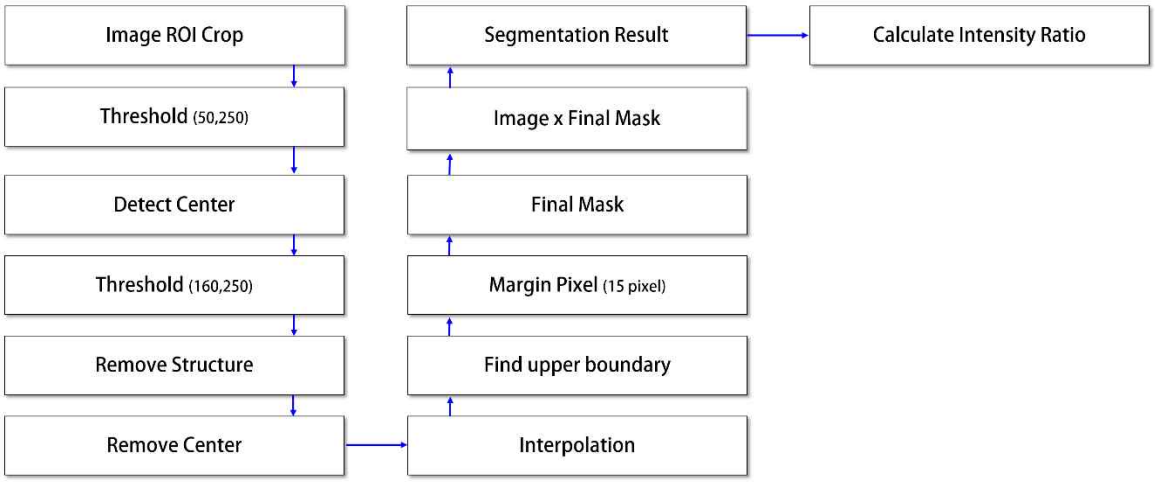

Figure 5. Automated mEZi quantification flowchart

4. Calibration Study-Determining the Relationship of the AM to MM macula EZ Intensity Quantification within a Representative Group of 160 Images Sets

To compare the mEZi quantification of AM and MM in different mEZi ranges, OCT images were obtained from three representative groups of different disease stage: normal (n = 40), mild-to-moderate glaucoma (n = 60), or severe glaucoma (n = 60). Output data for each images sets was the mEZi quantified by the AM and MM, and the results were directly compared.

5. Validation Study-Comparison of Compensated AM to MM macula EZ Intensity Quantification within a Second Representative Group of *n* = 33 Images Sets with Multiple (5) MM Quantification

To validate the algorithm, we considered values obtained by MM to be the ground truth. Thus, AM mEZi quantification were compared with the mean and range of repeatability (95% CI) derived from five separate repeated MM mEZi quantifications. For this validation study, a separate group of 33 representative images was used. The images in this group were from

normal (n = 11), mild-to-moderate glaucoma (n = 11) or severe (n = 11) glaucoma eyes. MM mEZi quantification was performed on all 33 images sets by the same operator (YKK) on five separate occasions at least 3 days apart. Correlation between the AM and MM quantification was assessed. AM quantification for each images sets were then compensated using the equation resulting from the linear regression of the difference versus average mEZi quantification from the calibration set. The number of images for which the compensated AM quantification fell outside of the 95% CI of the MM quantification was recorded and the potential reasons for disagreement were assessed.

6. Statistical Analysis

Comparison of the normally distributed mEZi within each study (i.e. calibration and validation) was performed by t-test. Between-method comparisons were performed with Deming regression and Bland-Altman plots. Deming regression is an errors-in-variables model which tries to find the line of best fit for a two-dimensional dataset. It differs from the simple linear regression in that it accounts for errors in observations on both the x- and the y-axis. Deming regression assesses the linearity between methods, with statistical significance demonstrated if the CI for the slope does not contain 1 and if the CI for the intercept does not include 0.[42] Bland-Altman plots are presented for visual representation of the agreement between methods. Statistical analysis was performed using the MedCalc software (version 12.1.3.0, Mariakerke, Belgium), and a P value less than 0.05 was considered statistically significant.

III. Results

Table 2 reports the mean ± standard deviation (SD) and range of mEZi quantification by each method for the normal, mild-to-moderate glaucoma, and severe glaucoma images sets used in the calibration and validation studies, respectively. These data confirm that the normal and glaucoma groups represent a range of mEZi and that the range is similar in both studies.

Table 2. Macular Ellipsoid Zone Intensity within the Normal, Mild-to-Moderate, and Severe Glaucoma Stage in the Calibration and Validation Studies by Quantification Method

	Calibration Study *(n = 160)*				Validation Study *(n = 33)*				
	MM		AM		MM*		AM†		
	Mean ± SD	Range	Mean ± SD	Range	Mean ± SD	Range	Mean ± SD	Range	*t* -Test
Normal	**4.08 ± 0.42**	3.31-5.19	**4.26 ± 0.43**	3.38-5.33	**4.12 ± 0.43**	3.75-5.09	**4.32 ± 0.40**	3.84-5.13	$P = 0.620$
Mild-to-moderate Glaucoma	**3.14 ± 0.43**	2.21-4.48	**3.24 ± 0.42**	2.26-4.55	**3.14 ± 0.36**	2.78-4.08	**3.23 ± 0.34**	2.86-4.17	$P = 1.000$
Severe Glaucoma	**2.38 ± 0.52**	1.02-3.40	**2.50 ± 0.51**	1.02-3.41	**2.36 ± 0.27**	1.89-2.87	**2.54 ± 0.26**	2.09-2.99	$P = 0.830$

* MM quantification in the validation study are the mean of five separate counting sessions.
† AM quantification in the validation study are compensated using the equation for the regression line generated in the calibration study.

1. Calibration of AM to MM EZ Intensity Quantification within an Initial Group of 160 Images Sets

The AM quantification was plotted versus MM quantifications for all 160 images sets in Figure 6. The relationship between AM (abscissa) and MM quantifications (ordinate) was AM = 0.0560 + 1.024 (MM) with an R^2 of 0.991 ($P < 0.001$, Deming regression). These data indicated that there was close correlation between AM and MM quantifications in images from normal eyes as well as through the complete range of mild-to-moderate to severe glaucomatous damage. A Bland-Altman plot (Figure 7) demonstrated an average difference of 0.13 mEZi (AM > MM) and the limits of agreement extended from -0.09 to +0.35 mEZi.

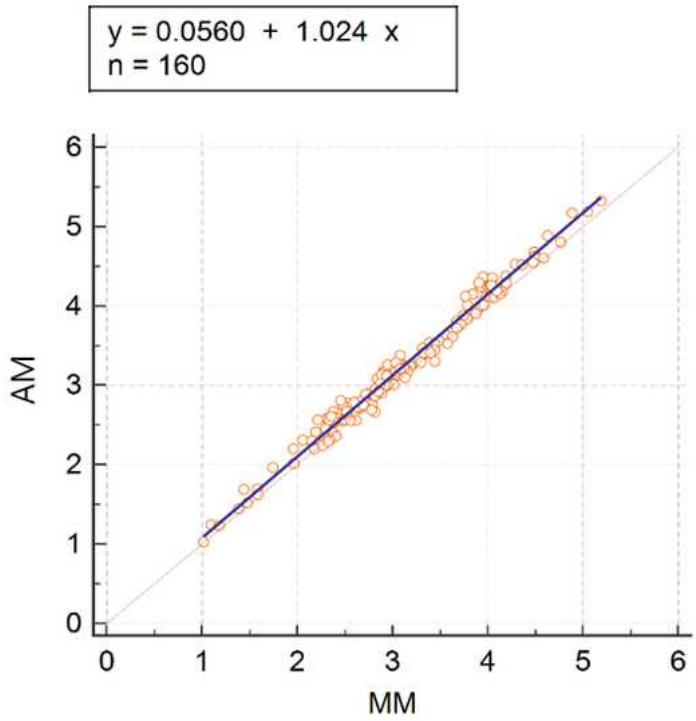

Figure 6. AM versus MM mEZi quantification in 160 images. The correlation produced an $R^2 = 0.991$ ($P < 0.001$). The relation of AM to MM quantification established by Deming regression is defined by the formula AM = 0.056 + 1.024 (MM) by the solid line.

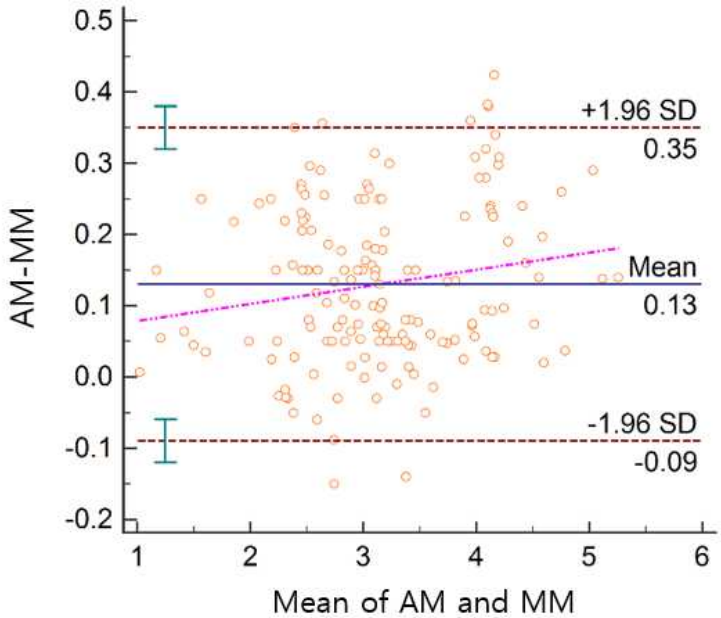

Figure 7. Bland-Altman plot for the 160 calibration images. The dashed red lines represent

the 95% limits of agreement between the AM and MM (-0.09 and +0.35).

2. Validation of the AM Calibration to MM Quantification within a Second Group of 33 Images Sets with Multiple Repeats (5) of MM Counts

The relationship between uncompensated AM quantification and the mean of five repeated MM counts for these 33 images sets was R^2 of 0.942 ($P < 0.001$, Deming regression). After AM quantification were compensated (by the regression from data in Figure 6), the mean ± SD of the MM quantification (3.14 ± 0.36 in mild-to-moderate glaucoma group; 2.36 ± 0.27 in severe glaucoma group) was not significantly different from the mean ± SD of the AM quantification (3.23 ± 0.34 in mild-to-moderate glaucoma group; 2.54 ± 0.26 in severe glaucoma group) used in this validation set (Wilcoxon singed rank test [$P = 0.110$ and 0.075, respectively]). Compensated AM quantification are plotted versus the mean of five MM quantification for each of the 33 images sets in Figure 8. Figure 9 shows the AM quantification fell within the 95% confidence interval of MM counts in 32 of the 33 images sets (96.97%). The mean ± SD difference between the MM and AM quantification for the 33 validation study images sets was 0.15 mEZi.

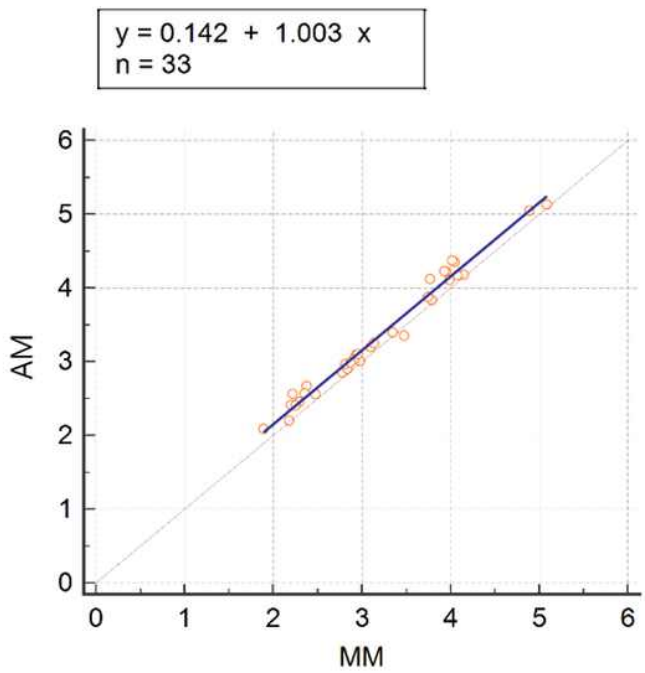

Figure 8. Validation of the calibration equation between AM and the mean of five MM mEZi quantification within a second group of 33 images. AM quantifications were compensated using the regression line equation established by the initial calibration study and compared to the mean of five repeated MM quantifications of each image. The solid line represents the result of the Deming regression; AM = 0.142 + 1.003 (MM), $R^2 = 0.942$, $P < 0.001$.

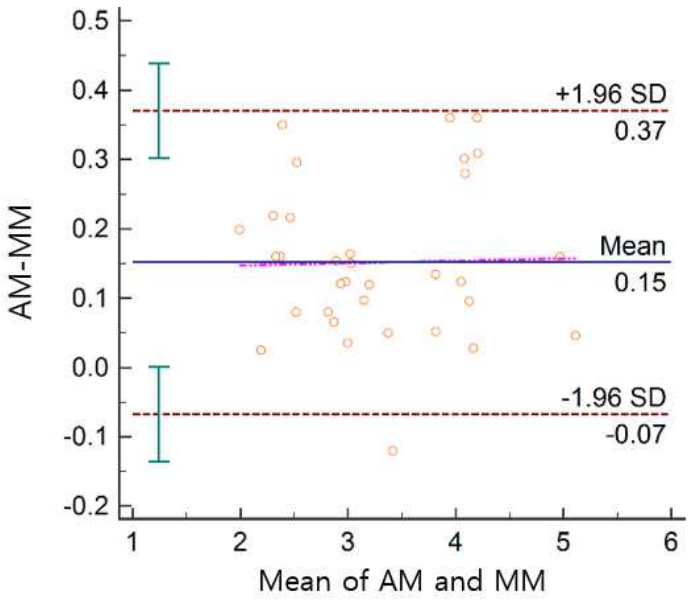

Figure 9. Bland-Altman plot for the 33 validation images. The dashed red lines represent the 95% limits of agreement between the AM and MM (-0.07 and +0.37).

IV. Discussion

The purpose of this study was to describe an automated algorithm and software application for quantification of mEZi, and to assess its performance relative to the manual method in SD-OCT images taken from normal and glaucomatous eyes with different disease stages. The automated method proved to be highly correlated to manual mEZi measurement in an initial calibration of 160 images. It also showed that its performance was similar to that of an experienced ophthalmologist in a validation set of 33 images counted five times each by demonstrating that its results fell within the ophthalmologist's 95% CI in 32 out of 33 images. Since the images in both sets demonstrated mEZi quantification ranging from normal to end-stage glaucoma, the results obtained showed that the study method achieved the requirements set forth at the start of the work: to develop an automated mEZi calculator that is applicable to all levels of glaucomatous damage and that is computationally robust and efficient.

In terms of performance, it took less than a minute to obtain a final mEZi value with AM in one SD-OCT image by the test system used for this study (MacBook Pro laptop, 2.2 GHz Core2 Duo, 3GB RAM; Apple, Cupertino, CA). Meanwhile, manual calculation of mEZi needed at least 5 minutes for the complete analysis of a single image. Analyzing a large number of images or wide range of areas by manual approach, thus, can be time consuming and error-prone. We expect that this automated mEZi analysis method will be applied in more large and diverse datasets, and foster further research on photoreceptor change in glaucoma as well as on evaluation of its clinical significance.

It is important to note that the method presented in this manuscript can be expanded to other diseases. EZ intensity is a known marker of severity in a number of diverse retinal pathologies such as age-related macular degeneration and inflammatory diseases.[10-13] However, due to the disruption of outer retinal layer by lesions such as drusen, reticular pseudodrusen, or hyperreflective foci in retinal diseases,[12] the detailed analysis protocol

might need modification and further validation. In addition, AM analysis can be easily modified to quantify intensities of outer retinal layers other than EZ, or to calculate intensities with other retinal layers as a reference value. The process to expand the software in these direction is already underway.

The present study's findings must be interpreted in light of its limitations. First, the number of sampling was not the same between the two methods: each meridian consisting of 20 retinal segments and one central segment in MM, but a total of 200 samples for AM. However, the EZ intensity reduction was proposed to occur as an overall retinal change during the glaucoma stage advancement rather than focal pathologic change.[43] Regardless of the number of analysis samples, therefore, the average values of the two methods would have shown a high agreement. Second, mEZi quantification using AM showed an analysis failure rate of 6.28%. In the OCT scans, the retinal layers are not always parallel to the horizontal plane of the image and had an irregularly curved shape. In those eyes with highly curved posterior structure such as in cases of high degree myopia, AM often failed to crop the ROI image. Future modifications in AM are planned to minimize analysis failure rate. Third, while compensation of the automated mEZi quantification was required to most fairly compare the performance of the AM to that of the MM in the validation study, it is not believed that the automated counts should be compensated in actual scientific application. Doing so would imply that the study manual mEZi analysis method is the gold standard and, thus, more accurate than the study's automated algorithm - something that is difficult, if not impossible, to determine yet. Therefore, future research will be needed to evaluate the accuracy of the two methods by comparing molecular changes in photoreceptors. Fourth, the performance of the described method depends on the quality of the input images like any other image processing algorithm. We carefully included OCT images with no artifacts and good image quality. Our results perhaps might not be directly applicable, therefore, to the OCT images with lower quality obtained in a real clinical setting.

In summary, this study presented a novel method for automated mEZi quantification in SD-OCT images. Study calibration and validation data indicate that its results are similar to manual mEZi calculation through a wide range of glaucomatous damage - from normal to end-stage glaucoma. We expect this automated mEZi quantification methods to be applied in various researches in ophthalmology.

REFERENCES

1. Quigley HA, Dunkelberger GR, Green WR. Retinal ganglion cell atrophy correlated with automated perimetry in human eyes with glaucoma. *American journal of ophthalmology.* 1989;107(5):453-464.
2. Osborne NN, Wood JP, Chidlow G, Bae J-H, Melena J, Nash MS. Ganglion cell death in glaucoma: what do we really know? *British Journal of Ophthalmology.* 1999;83(8):980-986.
3. Yücel YH, Zhang Q, Weinreb RN, Kaufman PL, Gupta N. Effects of retinal ganglion cell loss on magno-, parvo-, koniocellular pathways in the lateral geniculate nucleus and visual cortex in glaucoma. *Progress in Retinal and Eye Research.* 2003;22(4):465-481.
4. Panda S, Jonas JB. Decreased photoreceptor count in human eyes with secondary angle-closure glaucoma. *Investigative ophthalmology & visual science.* 1992;33(8):2532-2536.
5. Nork TM, Ver Hoeve JN, Poulsen GL, et al. Swelling and loss of photoreceptors in chronic human and experimental glaucomas. *Archives of ophthalmology.* 2000;118(2):235-245.
6. Velten IM, Korth M, Horn FK. The a-wave of the dark adapted electroretinogram in glaucomas: are photoreceptors affected? *British journal of ophthalmology.* 2001;85(4):397-402.
7. Holopigian K, Greenstein VC, Seiple W, Hood DC, Ritch R. Electrophysiologic assessment of photoreceptor function in patients with primary open-angle glaucoma. *Journal of glaucoma.* 2000;9(2):163-168.
8. Ho J, Sull AC, Vuong LN, et al. Assessment of artifacts and reproducibility across spectral- and time-domain optical coherence tomography devices. *Ophthalmology.* 2009;116(10):1960-1970.
9. Kiernan DF, Mieler WF, Hariprasad SM. Spectral-domain optical coherence tomography: a comparison of modern high-resolution retinal imaging systems. *American journal of ophthalmology.* 2010;149(1):18-31. e12.
10. Tao LW, Wu Z, Guymer RH, Luu CD. Ellipsoid zone on optical coherence tomography: a review. *Clinical & experimental ophthalmology.* 2016;44(5):422-430.
11. Cai CX, Locke KG, Ramachandran R, Birch DG, Hood DC. A comparison of progressive loss of the ellipsoid zone (EZ) band in autosomal dominant and x-linked retinitis pigmentosa. *Investigative ophthalmology & visual science.* 2014;55(11):7417-7422.
12. Gin TJ, Wu Z, Chew SK, Guymer RH, Luu CD. Quantitative Analysis of the Ellipsoid Zone Intensity in Phenotypic Variations of Intermediate Age-Related Macular DegenerationEZ Intensity in Age-Related Macular Degeneration. *Investigative ophthalmology & visual*

science. 2017;58(4):2079-2086.

13. Wu Z, Ayton LN, Guymer RH, Luu CD. Second reflective band intensity in age-related macular degeneration. *Ophthalmology.* 2013;120(6):1307-1308. e1301.
14. Spaide RF, Curcio CA. Anatomical correlates to the bands seen in the outer retina by optical coherence tomography: literature review and model. *Retina (Philadelphia, Pa).* 2011;31(8):1609.
15. Staurenghi G, Sadda S, Chakravarthy U, Spaide RF. Proposed lexicon for anatomic landmarks in normal posterior segment spectral-domain optical coherence tomography: the IN• OCT consensus. *Ophthalmology.* 2014;121(8):1572-1578.
16. Jaiswal M, Haelterman NA, Sandoval H, et al. Impaired mitochondrial energy production causes light-induced photoreceptor degeneration independent of oxidative stress. *PLoS biology.* 2015;13(7):e1002197.
17. Hoang Q, Linsenmeier R, Chung C, Curcio C. Photoreceptor inner segments in monkey and human retina: mitochondrial density, optics, and regional variation. *Visual neuroscience.* 2002;19(4):395-407.
18. Hood DC, Zhang X, Ramachandran R, et al. The inner segment/outer segment border seen on optical coherence tomography is less intense in patients with diminished cone function. *Investigative ophthalmology & visual science.* 2011;52(13):9703-9709.
19. Jonnal RS, Gorczynska I, Migacz JV, Azimipour M, Zawadzki RJ, Werner JS. The Properties of Outer Retinal Band Three Investigated With Adaptive-Optics Optical Coherence Tomography. *Investigative ophthalmology & visual science.* 2017;58(11):4559-4568.
20. Sundaram V, Wilde C, Aboshiha J, et al. Retinal Structure and Function in Achromatopsia: Implications for Gene Therapy. *Ophthalmology.* 2014;121(1):234-245.
21. Wu Z, Ayton LN, Guymer RH, Luu CD. Relationship between the second reflective band on optical coherence tomography and multifocal electroretinography in age-related macular degeneration. *Investigative ophthalmology & visual science.* 2013;54(4):2800-2806.
22. Masland RH. The neuronal organization of the retina. *Neuron.* 2012;76(2):266-280.
23. Jindahra P, Petrie A, Plant GT. Retrograde trans-synaptic retinal ganglion cell loss identified by optical coherence tomography. *Brain.* 2009;132(3):628-634.
24. Beatty R, Sadun A, Smith L, Vonsattel J, Richardson E. Direct demonstration of transsynaptic degeneration in the human visual system: a comparison of retrograde and anterograde changes. *Journal of Neurology, Neurosurgery & Psychiatry.* 1982;45(2):143-146.
25. Van Buren J. Trans-synaptic retrograde degeneration in the visual system of primates. *Journal of neurology, neurosurgery, and psychiatry.* 1963;26(5):402.

26. Ohno T. The possibility of centrifugal to the retina in the rat. *Cellular and Molecular Life Sciences.* 1980;36(12):1400-1401.
27. Wolter JR, Lund O. Reaction of centrifugal nerves in the human retina: Two weeks after photocoagulation. *American journal of ophthalmology.* 1968;66(2):221-232.
28. GILLS JP, Wadsworth JA. Retrograde transsynaptic degeneration of the inner nuclear layer of the retina. *Investigative ophthalmology & visual science.* 1967;6(4):437-448.
29. Herro AM, Lam BL. Retrograde degeneration of retinal ganglion cells in homonymous hemianopsia. *Clinical ophthalmology (Auckland, NZ).* 2015;9:1057.
30. Komáromy AM. *The Effect of Ganglion Cell Axotomy on Other Cells in the Porcine Retina*, University of Florida; 2002.
31. Xin D, Volgyi B, Amarillo Y, Bloomfield S. Polyaxonal amacrine cells in the rabbit retina. Paper presented at: INVESTIGATIVE OPHTHALMOLOGY & VISUAL SCIENCE2001.
32. Bleier R. Retrograde transsynaptic cellular degeneration in mammillary and ventral tegmental nuclei following limbic decortication in rabbits of various ages. *Brain Research.* 1969;15(2):365-393.
33. Jindahra P, Petrie A, Plant GT. The time course of retrograde trans-synaptic degeneration following occipital lobe damage in humans. *Brain.* 2012:534-541.
34. Johnson EC, Morrison JC. Friend or foe? Resolving the impact of glial responses in glaucoma. *Journal of glaucoma.* 2009;18(5):341.
35. Tezel G. Oxidative stress in glaucomatous neurodegeneration: Mechanisms and consequences. *Progress in Retinal and Eye Research.* 2006;25(5):490-513.
36. Prasanna G, Hulet C, Desai D, et al. Effect of elevated intraocular pressure on endothelin-1 in a rat model of glaucoma. *Pharmacological research.* 2005;51(1):41-50.
37. Spraul CW, Lang GE, Lang GK, Grossniklaus HE. Morphometric changes of the choriocapillaris and the choroidal vasculature in eyes with advanced glaucomatous changes. *Vision research.* 2002;42(7):923-932.
38. Yin ZQ, Millar TJ, Beaumont P, Sarks S. Widespread choroidal insufficiency in primary open-angle glaucoma. *Journal of glaucoma.* 1997;6(1):23-32.
39. Kur J, Newman EA, Chan-Ling T. Cellular and physiological mechanisms underlying blood flow regulation in the retina and choroid in health and disease. *Progress in retinal and eye research.* 2012;31(5):377-406.
40. Werner J, Keltner J, Zawadzki R, Choi S. Outer retinal abnormalities associated with inner retinal pathology in nonglaucomatous and glaucomatous optic neuropathies. *Eye.* 2011;25(3):279.

41. Choi SS, Zawadzki RJ, Lim MC, et al. Evidence of outer retinal changes in glaucoma patients as revealed by ultrahigh-resolution in vivo retinal imaging. *British Journal of Ophthalmology*. 2010:bjo. 2010.183756.
42. Deming WE. Chapter II. Simple illustractions of curve fitting. *Statistical adjustment of data.* 5th ed. New York, NY: Dover Publications; 2011.
43. Ha A, Kim YK, Jeoung JW, Park KH. Ellipsoid Zone Change According to Glaucoma Stage Advancement. *American journal of ophthalmology*. 2018;192:1-9.

국문초록

목적: 1) 녹내장 환자에서 황반부 타원체영역 반사강도(macular ellipsoid zone intensity, mEZi)를 수동 측정법(manual method, MM)을 통해 정량화하고 이를 정상안과 비교하고자 함. 2) mEZi 자동화 측정법(automated method, AM)을 개발하고, 기존 MM 과 비교 검증하고자 함.

방법: 71 명의 중등도 녹내장 환자(평균 나이, 58 ± 12 세), 71 명의 중증 녹내장 환자(60 ± 13 세), 그리고 51 명의 정상 대조군(60 ± 11 세)를 포함함. 모든 연구대상자들은 9 mm 길이의 고해상도 스펙트럼 영역 빛간섭단층촬영검사(spectral-domain optical coherence tomography, SD-OCT)를 황반부를 중심으로 총 4000 x 4000 μm 의 영역을 포함하는 수평 스캔과 수직 스캔검사를 시행 받음. 1) 총 37 명의 정상 대조군, 38 명의 시야결손 전 녹내장 환자, 39 명의 중등도 녹내장 환자, 그리고 36 명의 중증 녹내장 환자에서 MM 로 mEZi 를 측정함. 일원배치분산분석법(1-way analysis of variance with the Tukey post hoc test)을 통해 정상안 및 녹내장 중증도에 따라 mEZi 에 유의한 차이가 있는지를 비교 분석함. 2) 전체 연구 대상자를 질환군과 대조군 분포를 고려하여 측정군(Calibration group, n = 160)과 검증군(Validation group, n = 33)으로 나눔. AM 과 MM 측정법으로 얻은 mEZi 값의 분포를 Deming regression 을 이용해 비교검증하고 보정 공식을 산출 함. 검증군에서, 보정 공식으로 계산한 AM 측정법 결과가 MM 측정법으로 얻은 결과의 95% 신뢰도 구간에 위치하는지를 평가함.

결과: 1) 중증 녹내장 환자군에서 mEZi 는 중등도 녹내장 환자군보다 통계적으로 유의하게 낮았음(2.46 ± 0.38 vs. 3.15 ± 0.43, $P < 0.001$). 중등도 녹내장 환자군의 mEZi 는 시야결손 전 녹내장 환자군보다 유의하게 낮았음 (3.15 ± 0.43 vs. 3.86 ± 0.44, $P < 0.001$). 그러나, 시야결손 전 환자군의 mEZi 는 정상안과 통계적으로 유의한 차이를 보이지 않았음(3.86 ± 0.44 vs. 4.06 ± 0.40, $P = 0.751$). 2) AM 으로 얻은 mEZi 값은 MM 측정법으로 얻은 값과 유의한

선형 연관성을 보임 (측정군: R^2 = 0.991 및 P < 0.001, 검증군: R^2 = 0.942 및 P < 0.001). 33 명의 검정군 중에서 32 명(96.97%)에서 보정 공식으로 계산한 AM 결과가 MM 반복 측정으로 얻은 결과의 95% 신뢰도 구간에 위치함.

결론: 녹내장 환자에서 SD-OCT 이미지로 정량화 한 mEZi 는 정상인과 비교하여 유의하게 낮았으며, 진행된 녹내장에서는 그 감소 정도가 더 컸음. 이는 녹내장에서 광수용체 세포의 구조적 또는 기능적 변화가 동반될 가능성을 시사함. 또한, AM 으로 정량화 한 mEZi 는 다양한 녹내장 중등도에서 기존 MM 과 상관관계가 높음을 검증할 수 있었음.

.....

주요어: 황반부 타원체영역 반사강도, 자동화 측정, 보정 및 검증, 빛간섭단층촬영, 녹내장

학번: 2017-29480